

9. Conclusions and perspectives

9.1. Concluding remarks

This study, which deals with the problematical determination of long-term indoor ^{222}Rn progeny equilibrium factor using NTDs to well assess the annual effective dose in private homes and in workplaces, has led to the following conclusions:

1. The review of the most relevant parameters and processes affecting indoor ^{222}Rn and ^{220}Rn progeny concentrations has shown that their behaviour is very complex and that the equilibrium factor may change significantly from one house to another, depending on the geometry of the house, on the aerosol concentration, on the air mass movement, on the ambient conditions and on the inhabitants habits. Therefore, there is the need of measuring the long-term equilibrium factor indoors.
2. A detailed study of the measurement principles of airborne ^{222}Rn , ^{220}Rn and their progeny by means of NTDs, taking into account the range of variation of the parameters influencing their concentration, has shown that it is not possible for the existing methods to obtain the long-term equilibrium factor with an appropriate accuracy.
3. A new approach for long-term equilibrium factor determination from the measurement of airborne ^{222}Rn and its α -emitter daughters is presented in this PhD dissertation. This approach is based on the new concept of reduced equilibrium factor (F_{red}), which is defined as $F_{\text{red}} = \frac{0.105 C_{^{218}\text{Po}} + 0.380 C_{^{214}\text{Po}}}{C_{^{222}\text{Rn}}}$. We have shown that the equilibrium factor can be obtained with the best precision if proper optimisation of experimental conditions for the F_{red} measurement by means of NTDs is performed. In this method, assumptions about ventilation, aerosol attachment and deposition (attached and unattached) rates are not necessary.
4. We have designed a new passive, integrating and multi-component dosimeter to measure simultaneously the individual airborne concentration of ^{222}Rn , ^{220}Rn , ^{218}Po and ^{214}Po . It consists of: i) two Makrofol detectors, namely detectors A and B, which are

enclosed within two diffusion chambers — each one with different filter membrane — to measure indoor $^{222}\text{Rn}+^{220}\text{Rn}$ and ^{222}Rn , together with ii) two Makrofol detectors (C and D) that are kept in direct contact with air and that are electrochemically etched at different conditions to obtain the airborne ^{218}Po and ^{214}Po concentrations. The measurement method is based on the fact that the half-lives of ^{222}Rn and ^{220}Rn are different, that both isotopes have the same diffusion coefficient in a given medium and that the response of the Makrofol detector depends on the electrochemical etching conditions used.

5. From the slowing down spectrum of α -particles emitted by the airborne ^{222}Rn , ^{220}Rn and their progeny, and in order to avoid the plate-out peaks of these last, two α -energy windows of interest are chosen, one from 3.0 to 5.0 MeV for the detector A, B and C and another one from 6.3 to 7.5 MeV for the detector D. With these α -energy windows, the detector B lets the measurement of ^{222}Rn concentration. The concentration of ^{220}Rn can be obtained as a response difference of the detectors A and B. The reading of detector D allows the determination of the airborne ^{214}Po concentration. From this quantity and the information given by the detector C the airborne ^{218}Po concentration can be determined.
6. We have developed a Monte-Carlo computer code, called SIMAR, to obtain the sensitivity of each Makrofol detector, taking into account: (1) the Bethe-Bloch expression for the stopping power of heavily charged particles in a medium, (2) the behaviour of ^{222}Rn , ^{220}Rn and their progeny in the open air and within the diffusion chamber, and (3) the α -energy window response of each detector. The estimated sensitivity values have been validated by reproducing the response of an ideal detector, both in the free air and enclosed within a diffusion chamber.
7. The semi-automatic track counting system has been improved without any excessive cost, by connecting a photo video camera of an optical field area of $8.4 \times 6.3 \text{ mm}^2$ to a digital TV-graphic card and using a public domain Java image processing software, called ImageJ, for track analysis.
8. We have performed the initial phase of constructing a small exposure chamber, for both ^{222}Rn and ^{220}Rn , and we have set up an irradiation device to generate mono-energetic α -particles from 2 MeV up to 8 MeV with an α -energy resolution lower than 10%.
9. By studying the ^{222}Rn diffusion through some of the commercially available filters, we have shown that the glass fiber and the polyethylene are very appropriate for the

detectors A and B, respectively, to perform separate measurement of indoor ^{222}Rn and ^{220}Rn concentration.

10. We have confirmed experimentally using the irradiation device that the electrochemical etching conditions for the detectors A, B and C to generate an α -energy window response of [3.0 - 5.0] MeV are:

Etchant : KOH **6** M mixed with 50% ethanol
Temperature : 40 °C
Pre-etching duration : **4** h
Frequency : 3 kHz
Electric field strength : 33 kV cm⁻¹
ECE duration : **1.5** h

11. A detailed study of the main parameters influencing the electrochemical etching process of the Makrofol detectors have shown that the optimal etching conditions for the detector D to generate an α -energy window response of [6.3 - 7.5] MeV are:

Etchant : KOH **7.5** M mixed with 50% ethanol
Temperature : 40 °C
Pre-etching duration : **6** h
Frequency : 3 kHz
Electric field strength : 33 kV cm⁻¹
ECE duration : **1** h

12. The detectors A and B have been calibrated in pure ^{222}Rn atmospheres showing identical, consistent, and reproducible responses. The experimental sensitivity obtained for these detectors is very close to that given by the Monte-Carlo simulation.
13. With our passive, integrating and multi-component dosimeter, the a priori lower limit of detection can be estimated only for ^{222}Rn . The minimum detectable ^{222}Rn concentration is equal to 10 Bq m⁻³ for an eventual exposure time of 90 days.
14. By using well-control exposures in a reference laboratory, we have shown that the equilibrium factor values determined with our system agree with those obtained by active methods.

15. The results of an application indoors of our dosimeter in an inhabited Swedish single-family house suggest the usefulness of the method used in this study to carry out routine surveys for ^{222}Rn level measurements in private homes and in workplaces in order to estimate the associated annual effective dose received by the general public and the workers.

9.2. Future outlooks

In this PhD dissertation a novel approach has been proposed for long-term equilibrium factor determination from the measurement of ^{222}Rn and its α -emitter progeny (^{218}Po and ^{214}Po), and, therefore, new implications for future works have been opened. The main perspectives of this study are:

1. The sensitivity of the detector A in front of ^{220}Rn should be improved in order to extent its detectability to concentrations of the same order as those of ^{222}Rn . Further investigations of the parameters affecting the response of the other detectors should be also performed to optimise the system precision and to determine the sources or causes of errors.
2. A series of calibration exercises must be carried out in well-controlled ^{222}Rn and ^{220}Rn exposure facilities to complete the experimental determination of the sensitivities of the detectors A, B, C and D with respect to ^{222}Rn , ^{220}Rn and their α -emitter decay products. In addition, the response of our dosimeter at different equilibrium factors, ambient relative humidities and temperatures should be studied and evaluated.
3. The concept of the reduced equilibrium factor introduced in this work offers a lot of possibilities for the design and the development of new methods based on active or passive detectors for ^{222}Rn progeny equilibrium factor measurement.
4. With the passive integrating system set up in this study, it will be of great interest to carry out a national survey, in private homes and workplaces, in order to estimate the annual effective dose due to inhalation of indoor ^{222}Rn daughters and to identify those sites with high concentrations of ^{220}Rn .

A. Recoil energy determination from α -decay

Most of the heavy nuclei are energetically unstable against the spontaneous emission of a mono-energetic α -particle (or ${}^4\text{He}$ nucleus). The α -decay process can be written schematically as



where X and Y are the initial and the final nuclear species, A is the mass number of the nuclei X and Z its atomic number. For each distinct transition between initial and final nucleus, a fixed energy difference or Q -value characterises the α -decay as follows

$$Q = (m_X - m_Y - m_\alpha)c^2 \quad (\text{A.2})$$

where m_X , m_Y and m_α are the mass of the nuclei X , Y and the α -particle, respectively, and c is the light celerity.

In general, the kinetic energy of α -particle is usually lower than Q -value because of the recoil energy carried out by the residual nuclei Y . Thus, by applying the mass-conservation law, the kinetic energy of both α -particle and residual nuclei are given by

$$E_\alpha = \frac{m_Y}{m_Y + m_\alpha} Q = \frac{A-4}{A} Q \text{ and } E_Y = \frac{m_\alpha}{m_Y + m_\alpha} Q = \frac{4}{A} Q \quad (\text{A.3})$$

As the α -particle energy is a well known quantity for all the α -emitter radionuclide, the recoil energy can be estimated by the following expression

$$E_Y = \frac{4}{A-4} E_\alpha \quad (\text{A.4})$$

Table A.1 summarises the recoil energy of interest in the ${}^{222}\text{Rn}$ and ${}^{220}\text{Rn}$ chains.

Table A.1. The recoil energy of interest in the ^{222}Rn and ^{220}Rn chains.

X	E_α (MeV)	Y	E_Y (keV)
^{226}Ra	4.77	^{222}Rn	86
^{222}Rn	5.49	^{218}Po	101
^{218}Po	6.00	^{214}Pb	112
^{224}Ra	5.69	^{220}Rn	103
^{220}Rn	6.29	^{216}Po	117
^{216}Po	6.78	^{212}Pb	128
^{212}Bi	6.07	^{212}Po	115

B. Stopping power and range of α -particle in a medium

It is well known that the heavy ion (~ 8000 times the mass of the electron), when passing through matter loses, its energy predominantly via electronic interactions with the absorber atoms. The energy transferred in such collisions per unit of path length can be obtained from the well known Bethe-Bloch formula as follows (Bethe, 1930; Bloch, 1933)

$$\left(-\frac{dE}{dx}\right) (\text{MeV cm}^{-1}) = \frac{nZ_{\text{eff}}^2 e^4}{4\pi\epsilon_0^2 m_e v^2} \left[\ln \frac{2m_e v^2 w_{\text{max}}}{I^2(1-\beta^2)} - 2\beta^2 - \delta - U \right] \quad (\text{B.1})$$

where Z_{eff} is the effective charge of the heavy ion, v is its velocity, e is the electron charge, n is the electronic density of the absorber medium, ϵ_0 is the free space permittivity, m_e is the electron mass, I is the ionisation potential of the medium, β is the ion velocity relative to that of the light, w_{max} is the maximum energy transferred to the medium atoms, δ is a correction factor for polarisation of the medium, and U is a term that takes into account the participation of inner electron shells.

The most direct application of energy loss data is the determination of the ion ranges in medium materials. These last are regarded as having well defined ranges usually approximated to a straight line. The range of α -particles in a given medium can be calculated from the following integral

$$R(E) = \int_0^E \left(-\frac{dE}{dx}\right)^{-1} dE \quad (\text{B.2})$$

where E (MeV) is the ion energy. According to this equation, theoretical calculation of ion ranges within medium materials is not trivial. Instead, semi-empirical expressions, based on experimental data and guided by theory, are usually used.

In this study, we used the Srim-2000 code as a reference for the stopping power and range calculation. The range-energy results obtained for a given medium are fitted using the least-square minimisation method to establish the range-energy relationship. Figure

B.1 presents the range-energy data obtained for α -particles in Makrofol and in air using the Srim-2000 code. As shown in this figure, the α -particle range-energy relationships in both Makrofol and air are polynomial and the corresponding least-square fitting parameters obtained are

$$R_{\text{Makrofol}}(E) = 1.05 + 2.50E + 0.666E^2 \quad (R^2 = 0.998) \quad (\text{B.3})$$

$$R_{\text{air}}(E) = 0.12 + 0.297E + 0.07E^2 \quad (R^2 = 0.998) \quad (\text{B.4})$$

where the α -energy, E , is given in MeV and its corresponding range in Makrofol and in air are respectively given in μm and in cm. The uncertainties introduced by the fit were found to be less than 1%. These results differ from those obtained in a previous work of our group (Amgarou et al., 2001b) in which the Makrofol and air range-energy data calculated by the Srim-2000 code were adjusted to the common power function of the form $R(E) = aE^b$, suggested by the Bragg's rule and denoted by a dot line in Figure B.1. Nevertheless, as can be clearly seen in this figure, the polynomial adjustment is much more better for the Srim-2000 energy-range data than the function $R(E) = aE^b$.

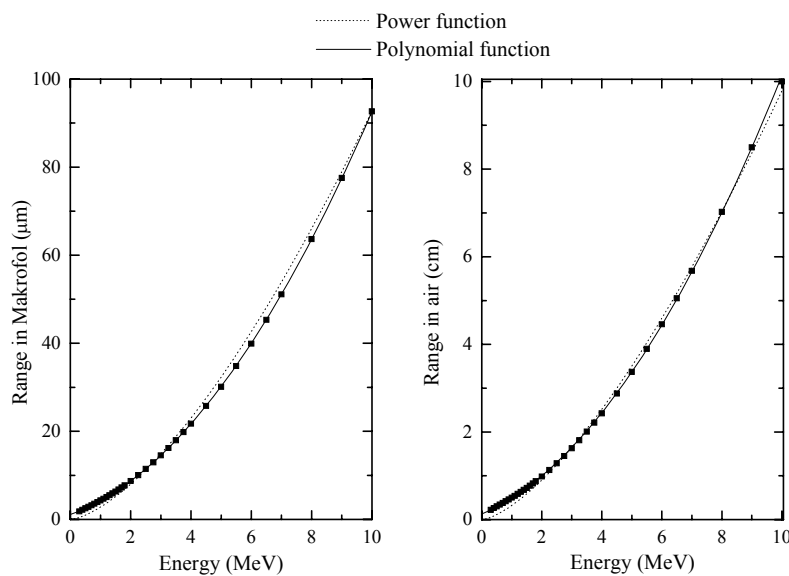


Figure B.1. Range-energy dependence for α -particles in Makrofol and in air.

C. A note on Monte-Carlo simulation

The name *Monte-Carlo* was applied for the first time by scientists working on the nuclear weapon project in Los Alamos, during the Second World War, to design a class of numerical methods based on the use of random numbers. A good review of the Monte-Carlo techniques and their application to simulate the physical systems could be found in Kalos and Whitlock (1986). The essential ingredient of the Monte-Carlo techniques is the numerical sampling of random variables with specified probability distribution functions (PDFs), which are positive function normalised to unity. Thus, considering a variable x that is randomly distributed in the interval (a, b) according to a given PDF, $p(x)$, we have

$$p(x) \geq 0 \text{ and } \int_a^b p(x) dx = 1 \quad (\text{C.1})$$

The cumulative distribution function of x is defined by

$$P(x) = \int_a^x p(x) dx \quad (\text{C.2})$$

This function increases monotonically from $P(a) = 0$ to $P(b) = 1$ and, therefore, has an (univariate) inverse function. The transformation $\xi = P(x)$ defines a new random variable, which takes values uniformly distributed in the interval $(0, 1)$; so that,

$$\xi = \int_a^x p(x) dx \quad (\text{C.3})$$

This equation is referred to as the sampling equation of the variable x . This procedure for random sampling is known as the inverse transform method; it is particularly adequate for PDFs, given by simple analytical expressions, such that the sampling equation can be solved analytically.

In general, random sampling algorithms are based on the computer generation of a pseudo-random number sequence between zero and unity from a given *seed* using a linear

congruential method. The name pseudo reflects the fact that the generated sequence is not truly random, since it is obtained from a deterministic algorithm. In this study, as a pseudo-random number generator algorithm we employed the subroutine `RANDOM_NUMBER` that is included in the Fortran 90 Scientific Function Package. This subroutine produces 32-bit floating point numbers uniformly distributed in the interval $(0, 1)$ and have a periodic sequence of the order of 10^{18} , which is virtually infinite for practical simulations.

Consider, for instance, the example of particle emission from a given radioactive source. The random numbers are then used to choose the coordinates and the direction of emission. By supposing that the variable Cartesian coordinate x is uniformly distributed in the interval (a, b) , we can write

$$p(x) = \frac{1}{b - a} \quad (\text{C.4})$$

Then, the sampling equation (C.3) leads to the well-known sampling formula

$$x = a + \xi(b - a) \quad (\text{C.5})$$

On the other hand, in order to simulate an isotropic particle emission (i.e., in all directions) from a radioactive source, the following angular distribution probability density is adopted

$$p(\theta, \varphi) \, d\theta \, d\varphi = \frac{1}{4\pi} \sin \theta \, d\theta \, d\varphi \quad (\text{C.6})$$

where θ and φ are, respectively, the zenith and azimuthal angles. Notice that $0 \leq \theta \leq \pi$ and $0 \leq \varphi \leq 2\pi$. Since these variables are independent, the term $p(\theta, \varphi)$ can be factorise as the product of two associated PDFs $f(\theta)$ and $g(\varphi)$, which are given by

$$f(\theta)d\theta = \frac{1}{2} \sin \theta \, d\theta \text{ and } g(\varphi) \, d\varphi = \frac{1}{2\pi} \quad (\text{C.7})$$

By choosing two independent random values, ξ_1 and ξ_2 , with uniform probability between 0 and 1, the initial direction of emission of a particle from an isotropic source can be generated by imposing that

$$\xi_1 = \int_0^\theta f(\theta)d\theta \text{ and } \xi_2 = \int_0^\varphi g(\varphi)d\varphi \quad (\text{C.8})$$

Solving these integrals, we finally obtain

$$\theta = \arccos(1 - 2\xi_1) \quad (\text{C.9})$$

$$\varphi = 2\pi\xi_2 \quad (\text{C.10})$$

References

- Ahmed N., Matiullah and Hussein A. J. A. (1998). Natural radioactivity in Jordanian soil and building materials and the associated radiation hazards. *J. Environ. Radioact.*, 39, pp. 9-22.
- Allen M. D. and Raabe O. G. (1985). Slip correction factor measurements of spherical solid aerosol particles in an improved Millikan apparatus. *Aerosol Sci. Technol.*, 4, pp. 269-286.
- Al-Najjar S. A. R., Bull R. K. and Durrani S. A. (1979). Electrochemical etching of CR-39 plastic: applications to radiation dosimetry. *Nucl. Tracks*, 3, pp. 169-183.
- Al-Najjar S. A. R., Oliveira A. and Piesch E. (1989). Extension of the α -particle energy range in polycarbonate using multiple step chemical and/or electrochemical etching. *Radiat. Prot. Dosim.*, 27, pp. 5-8.
- Amgarou K. (1997). Estimación del factor de equilibrio a partir de la determinación del grado de desequilibrio del ^{214}Po con detectores de Makrofol-DE. Master-Thesis, Universitat Autònoma de Barcelona (in Spanish).
- Amgarou K., Font Ll., Albarracín D., Domingo C., Fernández F. and Baixeras C. (2001a). Semi-automatic evaluation system for nuclear track detectors applied to radon measurements. *Radiat. Meas.*, 33, pp. 203-209.
- Amgarou K., Font Ll., Domingo C., Fernández F. and Baixeras C. (2001b). Simultaneous measurement of radon, radon progeny and thoron concentrations using Makrofol-DE detectors. *Radiat. Meas.*, 34, pp. 139-144.
- Andriamanatena R., Bacmeister G. U., Freyer K., Ghose R., Jönsson G., Kleis T., Treutler H. -C. and Enge W. (1997). Modelling of solid state nuclear track detector devices for radon measurements. *Radiat. Meas.*, 28, pp. 657-662.

- Baixeras C., Garcia I., Fernández F., Domingo C., Vidal-Quadras A. and Piesch E. (1991). Indoor radon concentration measurements in some Spanish houses and dwellings with a plastic nuclear track detectors. *Nucl. Tracks Radiat. Meas.*, 19, pp. 279-282.
- Baixeras C., Font Ll., Robles B. and Gutiérrez J. (1996). Indoor radon survey in the most populated areas in Spain. *Environ. Int.*, 22, pp. S671-S676.
- Baixeras C., Amgarou K., Font Ll., Domingo C. and Fernández F. (1999a). Determination of the long-term equilibrium factor indoors by means of Makrofol track-etched detectors. *Il Nuovo Cimento C*, 22, pp. 325-329.
- Baixeras C., Amgarou K., Font Ll. and Domingo C. (1999b). Long-term radon levels and equilibrium factor in some Spanish workplaces measured with a passive integrating detector. *Radiat. Prot. Dosim.*, 85, pp. 233-236.
- Baixeras C., Amgarou K., Font Ll., Domingo C. and Fernández F. (1999c). Measurement of ^{214}Po concentration in air using Makrofol-DE detectors. *Radiat. Meas.*, 31, pp. 313-318.
- Bednár J., Burgkhardt B. and Turek K. (1998). Registration efficiency of alpha particles in Makrofol treated by three-step chemical and electrochemical etching. *Radiat. Meas.*, 29, pp. 453-460.
- Bethe H. A. (1930). Theory of the passage of rapid corpuscular rays through matter. *Ann. Physik*, 5, pp. 235-400 (in German).
- Bloch F. (1933). Stopping power of atoms with many electrons. *Z. Physik*, 81, pp. 363-376 (in German).
- Bochicchio F., McLaughlin J. P. and Piermattei S. (1995). Radon in indoor air. in: *Indoor air quality and its impact on man. European Collaborative Action, Report EUR 16123.*
- Boletín Oficial del Estado (BOE) (2001). Reglamento sobre protección sanitaria contra radiaciones ionizantes. Real Decreto 783/2001, 178, pp. 27284-27393 (Spanish Legislation).
- Bojanowski R., Radecki Z., Campbell M. J., Burns K. I. and Trinkl A. (2001). Report on the intercomparison run for the determination of radionuclides in soils: IAEA-326 and IAEA-327. International Atomic Energy Agency (IAEA), Vienna, IAEA/AL/100.
- Bonetti R., Capra L., Chiesa C., Guglielmetti and A. Mibiorino C. (1991). Energy response of LR-115 cellulose nitrate to alpha-particle beams. *Nucl. Tracks Radiat. Meas.*, 18, pp. 321-324.

- Bricard J. (1977). Physique des aérosols II: nucléation, condensation, ions, électrisation et propriétés optiques. CEA Report, CEA-R-4831(2) (in French).
- Bruno R. C. (1983). Verifying a model of radon decay product behaviour indoors. *Health Phys.*, 45, pp. 471-480.
- Busigin A., Van Der Vooren A. W., Babcock J. C. and Phillips C. R. (1981). The nature of unattached RaA(^{218}Po) particles. *Health Phys.*, 40, pp. 333-343.
- Capra D., Silibello C. and Queirazza G. (1994). Influence of ventilation rate on indoor radon concentration: theoretical evaluation and experimental data in a test chamber. *J. Environ. Radioact.*, 24, pp. 205-215.
- Cheng Y. S., Allen M. D., Gallegos D. P., Yeh H. C. and Peterson K. (1988). Drag force and slip correction factor of aggregate aerosols. *Aerosol Sci. Technol.*, 8, pp. 199-214.
- Cheng Y. S., Chen T. R., Yeh H. C., Bigu J., Holub R., Tu K., Knutson E. O. and Falk R. (2000). Intercomparison of activity size distribution of thoron progeny and a mixture of radon and thoron progeny. *J. Environ. Radioact.*, 51, pp. 59-78.
- Chu K. D. and Hopke P. K. (1988). Neutralization kinetics for Polonium-218. *Environ. Sci. Tech.*, 22, pp. 711-717.
- Cliff K. D. (1990). UK National Radiological Board radon calibration procedures. *Journal of the National Institute of Standards and Technology*, 95, pp. 135-138.
- Chemical Rubber Company (CRC) (2001). *Handbook of Chemistry and Physics*, ed. Lide D. L., The CRC Press, 82th Edition.
- Cross F. T. (1988). Evidence of lung cancer from animal studies. in: *Radon and its decay products in indoor air*, eds. Nazaroff W. W and Nero A. V., John Wiley & Sons, pp. 373-404.
- Currie L. A. (1968). Limits for qualitative detection and quantitative determination: application to radiochemistry. *Anal. Chem.*, 40, pp. 586-593.
- Djeffal S., Lounis Z. and Allab M. (1997). Design of a radon measuring device based on the diffusion principle using LR-115 detector. *Radiat. Meas.*, 28, pp. 629-632.
- Doi M., Fujimoto K., Kobayashi S. and Yonehara H. (1994). Spatial distribution of thoron and radon concentration in the indoor air of a traditional Japanese wooden house. *Health Phys.*, 66, pp. 43-49.

- Dománski T., Chruscielewski W. and Zórawski A. (1984). Method of radon and decay products equilibrium factor measurement with the use of passive track detectors. *Radiat. Prot. Dosim.*, 8, pp. 231-238.
- Domingo C., Thompson A., O'Sullivan D., Baixeras C., Fernández F and Vidal-Quadras A. (1990). Long term ageing effect for energetic ultraheavy ion tracks in polycarbonate solid state nuclear track detectors. *Nucl. Instr. and Meth. B*, 51, pp. 253-262.
- Domingo C., Font J., Baixeras C. and Fernández F. (1996). Source abundances of ultra heavy elements derived from UHCRE measurements. *Radiat. Meas.*, 26, pp. 825-832.
- Dorrian M. D. (1997). Particle size distributions of radioactive aerosols in the environment. *Radiat. Prot. Dosim.*, 69, pp. 117-132.
- Dörschel B. and Guhr A. (1993). Measurement of the potential alpha energy concentration of radon daughters by means of a double chamber system and solid state nuclear track detectors. *Radiat. Prot. Dosim.*, 49, pp. 459-464.
- Dörschel B. and Piesch E. (1993). A new approach to estimating the equilibrium factor between radon and its daughters. *Radiat. Prot. Dosim.*, 48, pp. 145-151.
- Dörschel B. and Piesch E. (1994). Effect of varying unattached fraction of radon daughters on the measurement of the equilibrium factor using nuclear etched track detectors. *Radiat. Prot. Dosim.*, 54, pp. 41-45.
- Durrani S. A. and Bull R. K. (1987). *Solid state nuclear track detection: principles, methods and applications*. Pergamon Press.
- Durrani S. A. (1997). Alpha-particle etched track detectors. in: *Radon measurements by etched track detectors: application in radiation protection, earth sciences and the environment*, eds. Durrani S. A. and Ilic R., World Scientific, pp. 77-101.
- Fleischer R. L., Price P. B. and Walker R. M. (1975). *Nuclear tracks in solids: principles and applications*. University of California Press, Berkely.
- Fleischer R. L., Giard W. R., Mogro-campero A., Turner L. G., Alter H. W. and Gingrich J. E. (1980). Dosimetry of environmental radon: methods and theory for low-dose integrated measurements. *Health Phys.*, 39, pp. 957-962.
- Fleischer R. L. (1984). Theory of passive measurement of radon daughters and working levels by the nuclear track technique. *Health Phys.*, 47, pp. 263-270.

- Fleischer R. L., Turner L. G. and George A. C. (1984). Passive measurement of working levels and effective diffusion constants of radon daughters by the nuclear track technique. *Health Phys.*, 47, pp. 9-19.
- Font Ll. (1993). Determinació de la concentració de radó en l'interior d'edificis amb detectors plàstics de traces. Master-Thesis, Universitat Autònoma de Barcelona (in Catalan).
- Font Ll. (1997). Radon generation, entry and accumulation indoors. PhD Thesis, Universitat Autònoma de Barcelona.
- Font Ll., Baixeras C., Jönsson G., Devantier R., Mommin M. M., Albarracín D., Ghose R., Freyer K., Treutler H. C., Siedel J. -L. and Garcia R. (1999a). Continuous measurements of soil radon under regular field conditions. *Il Nuovo Cimento C*, 22, pp. 589-595.
- Font Ll., Baixeras C., Jönsson G., Enge W. and Ghose R. (1999b). Application of a radon model to explain indoor radon levels in a Swedish house. *Radiat. Meas.*, 31, pp. 359-362.
- Frank A. L. and Benton E. V. (1977). Radon dosimetry using nuclear track detectors. *Nucl. Track Det.*, 1, pp. 149-179.
- Frey G., Hoke P. K. and Stukel J. J. (1981). Effect of trace gases and water vapour on the diffusion coefficient of Po-218. *Science*, 211, pp. 480-481.
- Friedlander S. K. (2000). *Smoke, dust, and haze: fundamentals of aerosol dynamics*. Oxford University Press.
- Furuta S., Ito K. and Ishimori Y. (2000). A continuous radon progeny monitor with a vacuum vessel by alpha spectrometry. *Radiat. Prot. Dosim.*, 90, pp. 429-435.
- Gadgil A. J., Kong D. and Nazaroff W. W. (1992). Deposition of unattached radon progeny from enclosure flows. *Radiat. Prot. Dosim.*, 45, pp. 337-341.
- George A. C. and Breslin A. J. (1977). Measurements of environmental radon with integrating instruments. *Atomic Industrial Forum Uranium Mill Monitoring Workshop*, Albuquerque, New Mexico.
- George A. C. and Knutson E. O. (1994). Particle size of unattached radon progeny in filtered room air. *Radiat. Prot. Dosim.*, 56, pp. 119-121.
- George A. C. (1996). State-of-the-art instruments for measuring radon/thoron and their progeny in dwellings — a review. *Health Phys.*, 70, pp. 451-463.
- Goldstein S. D. and Hopke P. K. (1985). Environmental neutralisation of polonium-218. *Environ. Sci. Technol.*, 19, pp. 146-150.

- Gutiérrez J., Baixeras C., Robles B., Saez J. C. and Font Ll. (1992). Indoor radon levels and dose estimation in two major Spanish cities. *Radiat. Prot. Dosim.*, 45, pp. 495-498.
- Hadler J. C. and Paulo S. R. (1994). Indoor radon daughter contamination monitoring: the absolute efficiency of CR-39 taking into account the plateout effect and environmental conditions. *Radiat. Prot. Dosim.*, 51, pp. 283-296.
- Hadler J. C., Iunes P. J. and Paulo S. R. (1995). A possibility of monitoring indoor radon daughters by using CR-39 as an alpha-spectrometer. *Radiat. Meas.*, 25, pp. 609-610.
- Hafez A. -F. and Somogyi G. (1986). Determination of radon and thoron permeability through some plastics by track technique. *Nucl. Tracks*, 12, pp. 697-700.
- Harley N. H., Chittaporn P., Fisenne I. M. and Perry P. (2000). ^{222}Rn decay products as tracers of indoor and outdoor aerosol particle size. *J. Environ. Radioact.*, 51, pp. 27-35.
- Harley J. H. (1992). Measurement of ^{222}Rn : a brief history. *Radiat. Prot. Dosim.*, 51, pp. 13-18.
- Hassib G. M. (1979). A pre-electrochemical etching treatment to improve neutron recoil track detection. *Nucl. Tracks*, 3, pp. 45-52.
- Hatori T. and Ishida H. (1994). A continuous monitor for radon progeny and its unattached fraction. *Radiat. Prot. Dosim.*, 55, pp. 113-122.
- Howarth C. B. and Miles J. C. H. (2000a). Results of the 1998 European Commission intercomparison of passive radon detectors. European Commission, Directorate-General for Research, Report EUR 18835.
- Howarth C. B. and Miles J. C. H. (2000b). Results of the 1999 European Commission intercomparison of passive radon detectors. European Commission, Directorate-General for Research, Report EUR 19148.
- Huet C., Tymen G. and Boulaud D. (2001). Size distribution, equilibrium ratio and unattached fraction of radon decay products under typical indoor domestic conditions. *Sci. Total Environ.*, 272, pp. 97-103.
- Ibrahim N. (1999). Natural activities of ^{238}U , ^{232}Th and ^{40}K in building materials. *J. Environ. Radioact.*, 43, pp. 255-258.
- International Commission on Radiological Protection (ICRP) (1987). Lung cancer risk from indoor exposures to radon progeny. *Annals of the ICRP* 50, Pergamon Press.

- International Commission on Radiological Protection (ICRP) (1994). Protection against radon-222 at home and at work. *Annals of the ICRP* 65, Pergamon Press.
- Ilic R. and Sutej T. (1997). Radon monitoring devices based on etched track detectors. in: *Radon measurements by etched track detectors: application in radiation protection, earth sciences and the environment*, eds. Durrani S. A. and Ilic R., World Scientific, pp. 103-128.
- Izerrouken M., Skovarc J. and Ilic R. (1999). Low energy alpha particle spectroscopy using CR-39 detector. *Radiat. Meas.*, 31, pp. 141-144.
- Jacobi W. (1972). Activity and potential α -energy of ^{222}Rn and ^{220}Rn daughters in different air atmospheres. *Health Phys.*, 22, pp. 441-450.
- James A. C. (1988). Lung dosimetry. in: *Radon and its decay products in indoor air*, eds. Nazaroff W. W and Nero A. V., John Wiley & Sons, pp. 259-309.
- Jha G. (1982). Radon permeability of some membranes. *Health Phys.*, 42, pp. 723-725.
- Kalos M. H. and Whitlock P. A. (1986). *Monte Carlo methods: basics I*. John Wiley & Sons.
- Kies A., Biell A., Rowlinson L. and Feider M. (1996). Investigation of the dynamics of indoor radon and radon progeny concentration. *Environ. Int.*, 22, pp. S899-S904.
- Knoll G. F. (2000). *Radiation detection and measurement: third edition*. John Wiley & Sons, pp. 161-202.
- Knutson E., George A., Frey J. and Koh B. (1983). Radon daughter plateout. *Health Phys.*, 45, pp. 445-452.
- Knutson E. O. (1988). Modeling indoor concentrations of radon's decay products. in: *Radon and its decay products in indoor air*, eds. Nazaroff W. W and Nero A. V., John Wiley & Sons, pp. 161-202.
- Knutson E. O., George A. C. and Tu K. W. (1997). The graded screen technique for measuring the diffusion coefficient of radon decay products. *Aerosol Sci. Technol.*, 27, pp. 604-624.
- Kojima H. (1988). Experimental estimation of a recoil factor in alpha decay of RaA. *Res. Let. Atmos. Elec.*, 8, pp. 69-74.
- Kojima H., Abe S. and Fujitaka K. (1993). Semi-empirical estimation of deposition velocity of unattached radon daughters in a room. *Radiat. Prot. Dosim.*, 46, pp. 103-109.

- Kotrappa P., Bhanti D. P. and Raghunath B. (1976). Diffusion coefficients for unattached decay products of thoron — dependence on ventilation and relative humidity. *Health Phys.*, 31, pp. 378-380.
- Lembrechts J., Janssen M. and Stoop P. (2001). Ventilation and radon transport in Dutch dwellings: computer modelling and field measurements. *Sci. Total Environ.*, 272, pp. 73-78.
- Leonard B. E. (1996). High ^{222}Rn levels, enhanced surface deposition, increased diffusion coefficient, humidity, and air exchange effects. *Health Phys.*, 70, pp. 372-387.
- Lida T, Nurishi R. and Okamoto K. (1996). Passive integrating ^{222}Rn and ^{220}Rn cup monitors with CR-39 detectors. *Environ. Int.*, 22, pp. S641-S647.
- Limoto T. and Kurosawa R. (1996). A pulse-coincidence ^{220}Rn monitor with three time-gates. *Environ. Int.*, 22, pp. S1139-S1145.
- Ling C. (1993). The measurement of equilibrium factor for radon by SSNTD. *Nucl. Tracks Radiat. Meas.*, 22, pp. 293-296.
- Lück H. B. (1986). On tree initiation and propagation in electrochemical etching of particle tracks. *Nucl. Tracks Radiat. Meas.*, 11, pp. 17-23.
- Malet J., Michielsen N., Boulaud D. and Renoux A. (2000). Mass transfer of diffusive species with non constant in-flight formation and removal in laminar tube flow: application to unattached short-lived radon daughters. *Aerosol Sci. Technol.*, 32, pp. 168-183.
- Maniyan C. G., Haridasan P. P., Paul A. C. and Rudan K. (1999). Influence of thoron progeny on the formation of tracks in SSNTD films (LR-115-II). *Radiat. Prot. Dosim.*, 82, pp. 263-269.
- Maroni M. (1998). Health effects of indoor air pollutants and their mitigation and control. *Radiat. Prot. Dosim.*, 78, pp. 27-32.
- McLaughlin J. P. and Fitzgerald B. (1992). A new technique to measure the activities of short-lived radon progeny deposited on surfaces. *Radiat. Prot. Dosim.*, 45, pp. 115-118.
- McLaughlin J. P. and Fitzgerald B. (1994). Models for determining the response of passive alpha particle detectors to radon and its progeny in cylindrical detecting volumes. *Radiat. Prot. Dosim.*, 56, pp. 241-246.
- Mercer T. T. (1976). The effect of particle size on the escape of recoiling RaB atoms from particulate surface. *Health Phys.*, 31, pp. 173-174.

- Miles J. C. H., Algar R. A., Howarth C. B., Hubbard L. M., Risica S., Kies A. and Poffijn A. (1996). Results of the 1995 European Commission intercomparison of passive radon detectors. European Commission, Directorate-General XII, Report EUR 16949.
- Mirza S. M., Mirza N. M., Tufail M. and Ahmad N. (1993). Monte Carlo method to calculate volumetric activity to track density rate conversion coefficients for radon dosimetry. *Radiat. Prot. Dosim.*, 46, pp. 15-24.
- Mohammed A. (1999). Activity size distributions of short-lived radon progeny in indoor air. *Radiat. Prot. Dosim.*, 86, pp. 139-145.
- Monnin M. M. and Seidel J. L. (1997). Radon measurement techniques. in: Radon measurements by etched track detectors: application in radiation protection, earth sciences and the environment, eds. Durrani S. A. and Ilic R., World Scientific, pp. 51-74.
- Monnin M. and Seidel J. L. (1998). An automatic radon probe for earth science studies. *J. Appl. Geophys.*, 39, pp. 209-220.
- Mozzo P., Trotti F., Temporin A., Lanciai M., Predicatori F., Righetti F. and Tacconi A. (1996). α -Spectroscopy on CR-39 track detectors for the dosimetry of radon daughters. *Environ. Int.*, 22, pp. S595-S600.
- Nazaroff W. W., Moed B. A. and Sextro R. G. (1988a). Soil as a source of indoor radon: generation, migration, and entry. in: Radon and its decay products in indoor air, eds. Nazaroff W. W and Nero A. V., John Wiley & Sons, pp. 57-112.
- Nazaroff W. W., Doyle S. M., Nero A. V. and Sextro R. G. (1988b). Radon entry via potable water. in: Radon and its decay products in indoor air, eds. Nazaroff W. W and Nero A. V., John Wiley & Sons, pp. 131-157.
- Nazaroff W. W., Kong D. and Gadgil A. J. (1992). Numerical investigation of the deposition of unattached ^{218}Po and ^{212}Pb from natural convection enclosure flow. *J. Aerosol Sci.*, 23, pp. 339-352.
- Nazaroff W. W., Gadgil A. J. and Weschler C. J. (1993). Critique of the use of deposition velocity in modeling indoor air quality. in: Modeling of indoor air quality and exposure, eds. Niren L. Nagda, American Society for Testing and Materials, Philadelphia, pp. 81-104, ASTM STP 1205.
- Nero A. V. (1988). Radon and its decay products in indoor air: an overview. In radon and its decay products in indoor air, eds. Nazaroff W. W and Nero A. V., John Wiley & Sons, pp. 1-53.

- Nikezic D., Baixeras C. and Kostic D. (1995). Sensitivity determination and optimisation of a cylindrical diffusion chamber, for radon measurements, with a CR39 detector. *Nucl. Instr. and Meth. A*, 373, pp. 290-298.
- Nikezic D., Yu K. N., Cheung T. T. K., Haque A. K. M. M. and Vucic D. (2000). Effects of different lung morphology models on the calculated dose conversion factor from Rn progeny. *J. Environ. Radioact.*, 47, pp. 263-277.
- Nikolaev V. A. and Ilic R. (1999). Etched track radiometers in radon measurements: a review. *Radiat. Meas.*, 30, pp. 1-13.
- Nourreddine A., Azkour K., Benjelloun M., Boukhair A., Fahad M. and Pape A. (1999). Monte-Carlo detection probabilities for SSNTD application to uranium and thorium analysis in Moroccan phosphates. *J. Environ. Radioact.*, 42, pp. 101-107.
- National Research Council (NRC) (1991). Comparative dosimetry of radon in mines and homes. Washington D.C., National Academy Press.
- National Research Council (NRC) (1999). Health effects of exposure to radon: BEIR VI. Washington D.C., National Academy Press.
- O'Connor P. J., Gallagher V., Madden J. S., Van Den Boom G., McLaughlin J. P., McAulay I. R., Barton K. J., Duffy J. T., Muller R., Grimley S., Marsh D., Mackin G. and MacNiocail C. (1993). Assessment of the geological factors influencing the occurrence of radon hazard areas in a karstic region. Geological Survey of Ireland, Report Series RS93/2.
- Organisation for Economic Co-operation and Development: Nuclear Energy Agency (OECD/NEA) (1985). Metrology and monitoring of radon, thoron and their daughter products. Report by a Group of Experts of the OECD/NEA.
- Official Journal of the European Communities (OJEC) (1990). Protection of the public against indoor exposure to radon. Commission Recommendation 90/143/EURATOM, L80.
- Official Journal of the European Communities (OJEC) (1996). Basic safety standards for the protection of the health of workers and the general public against the dangers arising from ionizing radiation. Council Directive 96/29/EURATOM, 39, L159.
- Ortega X. and Vargas A. (1996). Characteristics and temporal variation of airborne radon decay progeny in the indoor environment in Catalonia (Spain). *Environ. Int.*, 22, pp. S149-S159.

- Papp Z. and Daróczy S. (1997). Measurement of radon decay products and thoron decay products in air by beta counting using end-window Geiger-Müller counter. *Health Phys.*, 72, pp. 601-610.
- Peter J. E. (1994). Analysis of radon and thoron daughter concentrations in air by continuous alpha spectroscopy. *Radiat. Prot. Dosim.*, 56, pp. 267-270.
- Phillips C. R., Khan A. and Leung H. M. Y. (1988). The nature and determination of the unattached fraction of radon and thoron progeny. in: *Radon and its decay products in indoor air*, eds. Nazaroff W. W and Nero A. V., John Wiley & Sons, pp. 203-256.
- Piesch E., Al-Najjar S. A. R. and Józefowicz K. (1991). The two-step electrochemical etching technique applied for polycarbonate track etched detectors. *Nucl. Tracks Radiat. Meas.*, 19, pp. 205-210.
- Pillai P. M. and Paul A. C. (1999). Studies on the equilibrium of ^{220}Rn (thoron) and its daughters in the atmosphere of a monazite plant and its environs. *Radiat. Prot. Dosim.*, 82, pp. 229-232.
- Planinic J. and Faj Z. (1989). The equilibrium factor F between radon and its daughters. *Nucl. Instr. and Meth. A*, 278, pp. 550-552.
- Planinic J. (1992). ^{222}Rn detection efficiency and sensitivity coefficient of the LR-115 nuclear track detector. *Health Phys.*, 62, pp. 356-358.
- Porstendörfer J. (1994). Properties and behaviour of radon and thoron and their decay products in the air. *J. Aerosol Sci.*, 25, pp. 219-263.
- Porstendörfer J. and Reineking A. (1999). Radon: characteristics in air and dose conversion factor. *Health Phys.*, 76, pp. 300-305.
- Raabe O. G. (1969). Concerning the interactions that occur between radon decay products and aerosols. *Health Phys.*, 17, pp. 177-185.
- Raes F., Janssens A. and Vanmarcke H. (1985). A closer look at the behaviour of radioactive decay products in air. *Sci. Total Environ.*, 45, pp. 205-218.
- Ramachandran T. V., Lalit B. Y. and Mishra U. C. (1987). Measurement of radon permeability through some membranes. *Nucl. Tracks Radiat. Meas.*, 13, pp. 81-84.
- Ramamurthi M. and Hopke P. K. (1989). On improving the validity of wire screen “unattached” fraction Rn daughter measurements. *Health Phys.*, 56, pp. 189-194.

- Reineking A. and Porstendörfer J. (1990). "Unattached" fraction of short-lived Rn decay products in indoor and outdoor environments: an improved single-screen method and results. *Health Phys.*, 58, pp. 715-727.
- Rogers V. C. and Neilson K. K. (1991). Correlations for predicting air permeabilities and ^{222}Rn diffusion coefficient of soils. *Health Phys.*, 61, pp. 225-230.
- Rogers V. C., Neilson K. K. and Holt R. B. (1995). Radon diffusion coefficients for aged residential concretes. *Health Phys.*, 68, pp. 832-834.
- Sarenio O. and Guhr A. (1991). A passive individual dosimeter for integrating measurements of the radon daughter contents in air. *Nucl. Tracks Radiat. Meas.*, 19, pp. 395-400.
- Schmidt V. and Hamel P. (2001). Measurements of deposition velocity of radon decay products for examination of the correlation between air activity concentration of radon and the accumulated Po-210 surface activity. *Sci. Total Environ.*, 272, pp. 189-194.
- Shi B. and Hopke P. K. (1991). Study of neutralization of ^{218}Po ions by small ion recombination in O_2 , Ar and N_2 . *Health Phys.*, 61, pp. 209-214.
- Shimo M. and Saito H. (2000). Size distribution of radon progeny aerosols in indoor and outdoor air. *J. Environ. Radioact.*, 51, pp. 49-57.
- Sima O. (2001). Monte Carlo simulation of radon SSNT detectors. *Radiat. Meas.*, 34, pp. 181-186.
- Sohrabi M. and Sadeghi M. (1991). Efficient detection and spectrometry of alphas from radon daughters in polycarbonate. *Nucl. Tracks Radiat. Meas.*, 19, pp. 421-422.
- Somogyi G., Paripás B. and Varga Zs. (1984). Measurement of radon, radon daughters and thoron concentration by multi-detector devices. *Nucl. Tracks Radiat. Meas.*, 8, pp. 423-427.
- Steinhäusler F. (1988). Epidemiological evidence of radon-induced health risks. in: *Radon and its decay products in indoor air*, eds. Nazaroff W. W and Nero A. V., John Wiley & Sons, pp. 311-371.
- Steinhäusler F. (1996). Environmental ^{220}Rn : a review. *Environ. Int.*, 22, pp. S1111-S1123.
- Stranden E. (1988). Building materials as a source of indoor radon. in: *Radon and its decay products in indoor air*, eds. Nazaroff W. W and Nero A. V., John Wiley & Sons, pp. 113-130.

- Swedjemark G. A. (1984). Temporal variation of the radon concentration indoors. *Radiat. Prot. Dosim.*, 7, pp. 255-258.
- Thatcher L. T., Fairchild W. A. and Nazaroff W. W. (1996). Particle deposition from natural convection enclosure flow onto smooth surfaces. *Aerosol Sci. Technol.*, 25, pp. 359-374.
- Tokonami S., Takahashi F., Limoto T. and Kurosawa R. (1997). A new device to measure the activity size distribution of radon progeny in low level environment. *Health Phys.*, 73, pp. 494-497.
- Tokonami S. (1999). Determination of the diffusion coefficient of unattached radon progeny with a graded screen array at the EML environmental chamber. *Radiat. Prot. Dosim.*, 81, pp. 285-290.
- Tokonami S. (2000). Experimental verification of the attachment theory of radon decay progeny onto ambient aerosols. *Health Phys.*, 78, pp. 74-79.
- Tommasino L. (1980). Solid dielectric detectors with breakdown phenomena and their applications in radioprotection. *Nucl. Instr. and Meth.*, 173, pp. 73-83.
- Tommasino L. and Harrison K. G. (1985). Damage track detectors for neutron dosimetry: registration and counting methods. *Radiat. Prot. Dosim.*, 10, pp. 207-217.
- Tommasino L. (1997). Track registration: etching and counting methods for nuclear tracks. in: *Radon measurements by etched track detectors: application in radiation protection, earth sciences and the environment*, eds. Durrani S. A. and Ilic R., World Scientific, pp. 103-128.
- Torrelles J., Baixeras C., Domingo C., Fernández F. and Vidal-Quadras A. (1988). Lexan polycarbonate response to relativistic gold ions. *Nucl. Tracks Radiat. Meas.*, 15, pp. 125-128.
- Tso M. W., Chor-yi Ng and Leung J. K. (1994). Radon release from building materials in Hong Kong. *Health Phys.*, 67, pp. 378-384.
- Tymen G., Robe M. C. and Rannou A. (1992). Measurements of aerosol and radon daughters in five radon houses. *Radiat. Prot. Dosim.*, 45, pp. 319-322.
- Tymen G., Kerouanton D., Huet C. and Boulaud D. (1999). An annular diffusion channel equipped with a track detector film for long-term measurements of activity concentration and size distribution of nanometer ^{218}Po particles. *J. Aerosol Sci.*, 30, pp. 205-216.

- United Nations Scientific Committee on the Effects of Atomic Radiation (UNSCEAR) (2000). Sources and effects of ionizing radiation. Vol. I: Sources, United Nations Publications, New York. Available in pdf format at: <http://www.unscear.org/2000vol1.htm>.
- Urban M. (1986). Passive one-element track etch dosimeter for simultaneous measurements of radon, thoron and decay products in air. *Nucl. Tracks Radiat. Meas.*, 12, pp. 685-688.
- Urban M. and Schmitz J. (1993). Radon and radon daughters metrology: basic aspects. European Commission, Directorate-General, Report EUR 14411, pp. 151-183.
- Vargas A. (2000). Contribución a la caracterización de aerosoles radiactivos derivados del radón. PhD Thesis, Universitat Politècnica de Catalunya (in Spanish).
- Voytchev M., Klein D., Chambaudet A., Georgiev G. and Iovtchev M. (1999). Applications of a silicon photodiode detector for radon progeny measurements. *Radiat. Meas.*, 31, pp. 375-378.
- Ward W. J. III, Fleischer R. L. and Mogro-Campero A. (1977). Barrier techniques for separate measurement of radon isotopes. *Rev. Sci. Instrum.*, 48, pp. 1440-1441.
- Willeke K. and Baron P. A. (1993). Aerosol measurement: principles, techniques and applications. John Wiley & Sons.
- Wong C. F. and Tommasino L. (1982). The frequency response of electrochemical etching. *Nucl. Tracks*, 6, pp. 25-34.
- Xu M., Nematollahi M., Sextro R. G., Gadgil A. J. and Nazaroff W. W. (1994). Deposition of tobacco smoke particles in low ventilation room. *Aerosol Sci. Technol.*, 20, pp. 194-206.
- Yamasaki T., Guo Q. and Lida T. (1995). Distributions of thoron progeny concentrations in dwellings. *Radiat. Prot. Dosim.*, 59, pp. 135-140.
- Yu K. N. (1993). The effects of typical covering materials on radon exhalation rate from concrete surfaces. *Radiat. Prot. Dosim.*, 48, pp. 367-370.
- Yu K. N., Cheung T., Guan Z. J., Young E. C. M., Mui B. W. N. and Wong Y. Y. (1999). Concentration of ^{222}Rn , ^{220}Rn and their progeny in residences in Hong Kong. *J. Environ. Radioact.*, 45, pp. 291-308.
- Yu K. N., Cheung T., Guan Z. J., Mui B. W. N. and Ng Y. T. (2000a). ^{222}Rn , ^{220}Rn and their progeny concentrations in offices in Hong Kong. *J. Environ. Radioact.*, 48, pp. 211-221.

- Yu K. N., Lau B. M. F., Guan Z. J., Lo T. Y. and Young E. C. M. (2000b). Survey of the Rn dose conversion factor for offices. *J. Environ. Radioact.*, 51, pp. 379-385.
- Yu K. N., Lau B. M. F., Guan Z. J., Lo T. Y. and Young E. C. M. (2001a). Brochial Rn dose for residences. *J. Environ. Radioact.*, 54, pp. 221-229.
- Yu K. N., Wong B. T. Y., Law J. Y. P., Lau B. M. F. and Nikezic D. (2001b). Indoor dose conversion coefficients for radon progeny for different ambient environments. *Environ. Sci. Technol.*, 35, pp. 2136-2140.
- Zhuo W., Lida T., Moriizumi J., Aoyagi T. and Takahashi I. (2001). Simulation of the concentrations and distribution of indoor radon and thoron. *Radiat. Prot. Dosim.*, 93, pp. 357-368.
- Ziegler J. T. and Biersak J. P. (1985). *The stopping and Range of ions in solids*. New York: Pergamon Press.

List of Figures

2.1	Decay diagram of ^{238}U series with the half-life of each radionuclide and the energies of α -emissions expressed in MeV.	7
2.2	Decay diagram of ^{232}Th series with the half-life of each radionuclide and the energies of α -emissions expressed in MeV.	8
2.3	Decay diagram of ^{235}U series with the half-life of each radionuclide and the energies of α -emissions expressed in MeV.	9
2.4	Schematic illustration of ^{222}Rn and ^{220}Rn emanation, transport and entry mechanisms from soil and buildings materials into indoor air — adapted from Knutson (1988). ^{226}Ra (^{224}Ra) atom, indicated by open circles, decays producing an α -particle and a ^{222}Rn (^{220}Rn) atom, which may end its recoil path at the point indicated by the solid circle. At A the parent atom is too deeply embedded within the grain for ^{222}Rn or ^{220}Rn atom to escape. At B and D the recoiling atom possesses sufficient energy after escaping the host to penetrate an neighbour grain. At C the ^{222}Rn or ^{220}Rn atom terminates its recoil in the pore water and, from there, it is readily transferred to the air-filled pore.	17
2.5	Schematic illustration of the ^{222}Rn and/or ^{220}Rn entry routes from soil into a house — adapted from (Font, 1997).	23
3.1	The basic processes influencing the indoor activity balance of ^{222}Rn and ^{220}Rn progeny — adapted from Knutson (1988).	41
3.2	Partitioning of indoor ^{222}Rn and ^{220}Rn decay product concentrations as a function of aerosol concentration within a reference room.	44
4.1	Schematic illustration of a chain scission in polymers caused by the passage of heavily charged particles — adapted from Durrani (1997).	52
4.2	Application of the Huygens principle to explain the latent track formation within polymer detectors.	53
4.3	The evolution of an etch pit profile with prolonged chemical etching — adapted from Durrani and Bull (1987).	54
4.4	Example of the tree-type damage tracks induced by the plutonium α -emissions in CR-39 — adapted from Tommasino (1997).	56

5.1	Illustration of the build-up and the cooling-off of ^{222}Rn concentration inside the diffusion chamber.	67
5.2	^{222}Rn progeny equilibrium factor vs. the ^{218}Po , ^{214}Pb and ^{214}Po disequilibrium degrees and of the ratio f_T assuming all the possible values for the free parameters λ_a , λ_v , λ_d^u and λ_d^a	70
5.3	^{222}Rn progeny equilibrium factor, $F_{^{222}\text{Rn}}$, as a function of the corresponding reduced equilibrium factor, $F_{\text{Red}} = 0.105 f_{^{218}\text{Po}} + 0.380 f_{^{214}\text{Po}}$, assuming all the possible values for the free parameters λ_a , λ_v , λ_d^u and λ_d^a . The values of the linear fitting parameters are given in the text.	74
5.4	^{220}Rn progeny equilibrium factor vs. the ^{212}Pb and ^{212}Bi disequilibrium degrees assuming all the possible values for the free parameters λ_a , λ_v , λ_d^u and λ_d^a	74
5.5	Frequency distribution in % of f_i^u , f_i^a , f_i^d , f_i , and F values obtained for ^{222}Rn progeny assuming all the possible values for the free parameters λ_a , λ_v , λ_d^u and λ_d^a . Data of these curves have been fitted to a log-normal distribution.	75
5.6	Frequency distribution in % of f_i^u , f_i^a , f_i^d , f_i , and F values obtained for ^{220}Rn progeny assuming all the possible values for the free parameters λ_a , λ_v , λ_d^u and λ_d^a . Data of these curves have been fitted to a log-normal distribution.	76
5.7	Slowing down spectrum in arbitrary units due to ^{222}Rn (A) and ^{220}Rn (B) α -emitter progeny in air and the corresponding peaks of the plate out effect on the detector surface. The coloured area shows the α -energy window response necessary for the NTDs to measure the airborne ^{214}Po concentration.	79
5.8	The design of the passive integrating system used to measure ^{222}Rn and its α -emitter progeny in the presence of ^{220}Rn	80
6.1	Flow chart of the SIMAR program.	87
6.2	Schematic illustration of α -particle registration with electrochemical etched Makrofol detectors.	88
6.3	Representation of the α -emission in the considered airspace.	90
6.4	The effective volumes of ^{222}Rn , ^{220}Rn and their α -active progeny obtained for the α -energy window [3.0 - 5.0] MeV, the black line illustrates the cross-section between the effective volume and the hemispherical housing in the case of detectors A and B.	92
6.5	The effective volume of ^{222}Rn , ^{220}Rn and their α -active progeny obtained for the α -energy window [6.3 - 7.5] MeV.	92
6.6	Enclosed SBD within the FzK diffusion chamber.	95
6.7	Typical α -spectrum measured with the SBD inside the FzK diffusion chamber in a ^{222}Rn -rich atmosphere.	96
6.8	Computed α -energy distributions of ^{222}Rn and its progeny as well as the resulting α -spectrum for an ideal detector within the FzK diffusion chamber. FD, LD and DD are defined in the text.	96

7.1	Elements of the electrochemical etching equipment: (1) the high alternative voltage/frequency generator, (2) the digital frequency-meter with a frequency-voltage-current selector, (3) the electric stove, (4) the security device, and (5) the modular etching cell system.	100
7.2	Schematic illustration of the modular cell system used for electrochemical etching of the Makrofol detectors.	101
7.3	A typical image of electrochemically etched Makrofol detectors as captured by the new semi-automatic system using an optical field area of $8.4 \times 6.3 \text{ mm}^2$	103
7.4	Illustration of the procedures used by the ImageJ program to evaluate electrochemically etched Makrofol detectors. By defining automatically the lower and upper grey-level thresholds (see the bottom right dialog box), the tracks are isolated and marked in red on the corresponding image screen (high left dialog box). The results of track morphology measurements are listed in the program menu window (high right dialog box). If required, additional histogram of the track area distribution can also be displayed (bottom left dialog box).	105
7.5	Response of the new and the old semi-automatic systems for track evaluation of electrochemically etched Makrofol detectors with respect to the manual counting. The error bars correspond to one standard deviation.	106
7.6	Experimental arrangement for the ^{222}Rn facility test developed in the present work.	108
7.7	An example of ^{222}Rn concentration built-up inside the exposure chamber together with the subsequent environmental conditions as measured by the Prassi monitor and the weather station, respectively.	109
7.8	Schematic illustration of the device used to generate the $^{212}\text{Bi}/\text{Po}$ source.	110
7.9	Measured α -spectrum of the ^{241}Am source by the multichannel pulse analyser at different source-to-detector distances. The peaks of interest have been fitted to a normal distribution.	111
7.10	Measured α -spectrum of the $^{212}\text{Bi}/\text{Po}$ source by the multichannel pulse analyser at different source-to-detector distances. The peaks of interest have been fitted to a normal distribution.	112
7.11	Energy-distance curves obtained for both the ^{241}Am and $^{212}\text{Bi}/\text{Po}$ sources. The error bars correspond to one standard deviation.	113
8.1	Experimental set-up used to determine the ^{222}Rn and ^{220}Rn diffusion constants through filters.	117
8.2	The counting rate evolution of the Clipperton probes with and without the polyethylene filter inside the small exposure chamber. The dotted line shows the time needed to reach the steady-state equilibrium.	117
8.3	Bulk etch rate (v_B) as a function of the etchant molarity at different values of % ethanol and etching temperature. The horizontal dotted lines indicate the interval of the required optimum bulk etch rates (between $7 \mu\text{m h}^{-1}$ and $8 \mu\text{m h}^{-1}$).	119

8.4	The removed layer as a function of the chemical etching duration, t_{CE} , using as etchant a solution 7.5 M KOH mixed with 50 % ethanol and an etching temperature of 40 °C. The solid line is a least-square adjustment of the data.	120
8.5	Electrochemical etched Makrofol efficiency as a function of the energy of the incident α -particles at different pre-etching times. The CE and ECE conditions are given in the text.	121
8.6	The low and upper energy thresholds of electrochemical etched Makrofol detectors as a function of the pre-etching time. The CE and ECE conditions are given in the text.	122
8.7	Calibration curve for the detector A against pure ^{222}Rn atmospheres.	124
8.8	Calibration curve for the detector B against pure ^{222}Rn atmospheres.	125
8.9	The relative standard deviation of the detectors A, B, C and D as a function of the net track density.	127
B.1	Range-energy dependence for α -particles in Makrofol and in air.	140

List of Tables

2.1	Physical properties of radon.	6
2.2	Decay constants, λ_i , and potential α -energy per atom, $E_{p,i}$, and per Bq of activity, $\frac{E_{p,i}}{\lambda_i}$, of the short-lived ^{222}Rn and ^{220}Rn daughters.	12
2.3	Traditional units and their equivalents in the SI accepted units.	14
2.4	Summary of the dose conversion factors for ^{222}Rn and ^{220}Rn progeny at private homes and workplaces.	15
2.5	Typical values and normal range of variation for the outdoor concentration, the soil volume-specific entry rate, the building material exhalation rate and the predicted indoor concentrations for ^{222}Rn and ^{220}Rn	26
3.1	Typical range of variation and baseline values of the indoor ventilation, attachment and deposition (airborne-unattached and aerosol-attached) rates.	43
4.1	Relative Standard Deviation (RSD) from the <i>true</i> annual average of different sampling periods (Swedjemark, 1984).	50
5.1	The comparison between the equilibrium factors obtained from the Reineking and Porstendörfer (1990) measurements of ^{222}Rn and its progeny concentrations in different German houses and those estimated from Equation (5.14).	72
5.2	The geometric means and the ranges of variation of f_i^u , f_i^a , f_i^d , f_i , and F values obtained for ^{222}Rn and ^{220}Rn progeny assuming all the possible values for the free parameters λ_a , λ_v , λ_d^u and λ_d^a as well as their geometric standard deviations (σ_g) and the corresponding correlation factors (R^2) of the fitted curves.	78
6.1	Characteristics of α -emissions ^{222}Rn , ^{220}Rn and their progeny and the calculated $\varepsilon_{m,n}^v$ and $\varepsilon_{m,n}^d$ values for the detectors A, B, C and D.	93
6.2	Comparison of the SIMAR program predictions with analytical method for an open ideal detector.	95
7.1	Reference α -energies used for the Makrofol detector irradiation.	113

8.1	Results of ^{222}Rn and ^{220}Rn diffusion coefficient in some filters together with the estimated delay time and the discrimination factor for the FzK diffusion chamber.	116
8.2	Characteristics of the exposure facilities as well as the relation of sets and measurement techniques used to calibrate the detector A against ^{222}Rn . . .	123
8.3	Results of simultaneous irradiation of the detectors A and B to ^{222}Rn and ^{220}Rn under different values of their exposures.	130
8.4	The comparison between the values of ^{222}Rn progeny equilibrium factor obtained by our passive integrating system and those given by the NRPB active monitor.	131
8.5	Results from indoor exposure of our passive integrating system in a Swedish house.	132
A.1	The recoil energy of interest in the ^{222}Rn and ^{220}Rn chains.	138